Available online at www.sciencedirect.com

International Journal of Mass Spectrometry 244 (2005) 50–59

www.elsevier.com/locate/ijms

A selected ion flow tube study of the reactions of H_3O^+, NO^+ and $O_2^{\bullet+}$ with methyl vinyl ketone and some atmospherically important aldehydes

E. Michel[a], N. Schoon[b,*], C. Amelynck[b], C. Guimbaud[a], V. Catoire[a], E. Arijs[b]

[a] *Laboratoire de Physique et Chimie de l'Environnement, Université d'Orléans, 3a Avenue de la Recherche Scientifique, 45071 Orléans Cedex 2, France*
[b] *Belgian Institute for Space Aeronomy, Ringlaan 3, B-1180 Brussels, Belgium*

Received 8 February 2005; accepted 12 April 2005

Abstract

The rate constant and product ion distribution of the reactions of H_3O^+, NO^+ and $O_2^{\bullet+}$ with methyl vinyl ketone (MVK), methacrolein (MaCR), pivaldehyde, 2-methyl-butanal, glyoxal, *o*-, *m*- and *p*-tolualdehyde have been investigated at 150 Pa and 297 K using a selected ion flow tube (SIFT). All reactions, except the NO^+/glyoxal reaction, proceed at a rate close to the collisional rate, calculated with the Su and Chesnavich model, using the polarizability and electric dipole moment of the compounds derived from quantum chemical calculations.

All H_3O^+ reactions proceed by proton transfer, non-dissociative for all compounds, except for 2-methyl-butanal, where two minor channels resulting from fragmentation after protonation are observed.

Association is the only pathway in the NO^+/MVK and NO^+/glyoxal reaction. Hydride ion transfer is the major process occurring in all the other NO^+ reactions. Elimination of CHO for pivaldehyde and association for MaCR are also non-negligible channels in their reaction with NO^+.

All $O_2^{\bullet+}$ reactions result in the parent cation by charge transfer and in at least one fragment ion.

Hydration of the product ions has been investigated by adding water vapor in the reaction zone. A method is proposed to derive the three-body association rate constants of the product ions with water and to estimate the rate constants of the reactions of the hydrated precursor ions $H_3O^+\cdot H_2O$ and $NO^+\cdot H_2O$ with the reactants.

Keywords: SIFT; Ion/molecule reactions; Aldehydes; Methyl vinyl ketone; Proton transfer; Charge transfer; Hydride ion transfer

1. Introduction

Aldehydes and other carbonyl compounds are widespread chemicals, which play an important role in the chemistry of the polluted troposphere. They can contribute to the formation of tropospheric ozone through their photo-chemistry in the gas phase [1] and take part in the generation of secondary aerosols through heterogeneous processes [2]. On local scale, aldehydes are toxic pollutants for human health [3,4].

Carbonyl compounds and aldehydes are introduced in the atmosphere by several antropogenic and natural sources. They are emitted from combustion processes of fossil fuels, industrial processes, waste disposal and biomass burning [5–7]. In addition, they arise as secondary pollutants from the photo-oxidation of volatile organic hydrocarbons, emitted in the atmosphere by industrial and biologic processes [8–10]. They can also be produced directly by various vegetation forms [11,12].

Aldehydes have been detected in the environment by a variety of techniques, based upon Fourier transform infrared spectroscopy, differential absorption in the near UV and GC–MS [8].

A very successful technique, which has recently been used for their measurement, is proton transfer reaction-mass spectrometry (PTR-MS) [13], which is based upon the mass spec-

---

* Corresponding author. Tel.: +32 2373 0391; fax: +32 2374 8423.
E-mail address: Niels.Schoon@bira-iasb.oma.be (N. Schoon).

1387-3806/$ – see front matter © 2005 Elsevier B.V. All rights reserved.
doi:10.1016/j.ijms.2005.04.005

trometric detection of the product ions generated from the reaction of the trace gas to be detected with H_3O^+ ions. A similar technique, which may be somewhat less sensitive, but which may allow a better identification of the chemicals to be measured, is the selected ion flow tube-mass spectrometry (SIFT-MS) method, developed and applied by Smith and co-workers for the measurement of a number of organic compounds [14–18]. In the latter method, not only the products of the reaction of the H_3O^+ ion with the compound to be detected are measured, but also the products of the reactions of NO^+ and $O_2^{\bullet+}$ ions.

The application of PTR-MS and SIFT-MS techniques, however, requires the knowledge of the kinetic and mechanistic data (reaction rate constants and product ion distribution) of the ion/molecule reactions involved.

Such data have been measured for several chemicals in the laboratory [19] and have recently been extended systematically by Španěl and co-workers to set-up a database of kinetic and mechanistic data for the detection of several organic compounds, including some aldehydes and ketones [20–22]. Although the existing database is quite extensive, some data are still missing, especially for some important atmospheric volatile compounds.

In this work, we have performed a study to extend the database to glyoxal, methacrolein (MaCR), methyl vinyl ketone (MVK), *o*-, *m*- and *p*-tolualdehyde.

The dicarbonyl compound glyoxal is formed in the atmosphere as a result of the photo-oxidation (reaction with OH) of toluene [23], which is an aromatic compound emitted in the atmosphere by automobile exhaust. Glyoxal is also a product of the photo-oxidation of other aromatic compounds [24–26] and of some biogenic species such as isoprene [27] and α-pinene [28]. Glyoxal is also believed to contribute significantly to the yield of secondary aerosols [2].

Methyl vinyl ketone and methacrolein are two major products, formed by the oxidation of isoprene (one of the major biogenic volatile organic compounds) by hydroxyl radicals and ozone, and minor products of the reaction of isoprene with NO_3 radicals [9].

The aromatic aldehydes *o*-, *m*- and *p*-tolualdehyde are emitted into the atmosphere as pollutants from motor vehicles [29,30] and are also produced in the atmosphere from the oxidation of xylenes [24,26,31]. Xylenes are released to the atmosphere from industrial sources, such as chemical plants, and from automobile exhaust.

In addition to these six compounds, reviewed above, we have added to our study the ion/molecule reactions of H_3O^+, NO^+ and $O_2^{\bullet+}$ with pivaldehyde and 2-methyl-butanal, two other atmospherically important aldehydes.

Apart from giving the information required for in situ detection of these compounds through SIFT-MS, our present data also give information for PTR-MS applications.

When SIFT-MS is used to identify and to quantify trace gases in various applications (such as environmental or breath analysis) the samples are generally “humid”. Therefore, it is essential to know if the ionic products of the H_3O^+, NO^+ and $O_2^{\bullet+}$ reactions associate with water and if the hydrates of the precursor ions also react with the trace gases under consideration. The formation of hydrates of the ionic products has thus also been studied here by introducing water vapor into the flow tube. Three-body association rate constants for the protonated products (see Section 3.2.1) and reaction rate constants for $H_3O^+{\cdot}H_2O$ and $NO^+{\cdot}H_2O$ with the reactants (see Section 3.1) have been derived, using a method described in Appendix A.

2. Experimental

Measurements are performed with a selected ion flow tube similar to the original design by Smith and Adams [32]. Since a detailed description of the equipment has been given in a previous publication [33], only a brief review of the instrument is given here.

The precursor ions H_3O^+, NO^+ and $O_2^{\bullet+}$ are generated in a microwave discharge in a mixture of air and water vapor at a total pressure of 20 Pa. By a set of electrostatic lenses ions are extracted from the discharge into a differentially pumped quadrupole mass spectrometer, which selects the appropriate ion. The mass selected ions are then injected into a 51 cm long flow tube with inner diameter of 4 cm, where they are convectively transported by a helium buffer gas flow. The reactant gas is introduced through a ring-shaped inlet, located 23.7 cm downstream from the injection point of the ions. At the downstream end of the flow tube ions are sampled through a 0.4 mm hole and introduced into the quadrupole analyzer, where they are filtered according to their mass to charge ratio. Ions are detected by an electron multiplier and the resulting signal is treated by pulse counting techniques.

All measurements were performed at 150 Pa and 297 K.

Ion/molecule reaction rate constants *k* were derived from the logarithmic decay $\ln(I/I_0) = -kt[X]$ of the source ion current *I* versus the concentration of the reactant neutral $[X]$ in the flow tube and from the residence time *t* of the ions in the flow tube, which can be measured separately.

The reactant neutral is diluted in helium in a volume calibrated glass container. The concentration of this reactant in the flow tube was varied by regulation of the flow rate from this glass container into the flow tube by means of a heated (315 K) needle valve. The reactant gas flow was inferred from the pressure decay versus time in the glass container. The concentration $[X]$ of the reactant was derived from the simultaneous measurement of the main carrier gas flow and of the pressure in the flow tube. In this way, the absolute reaction rate constants *k* of H_3O^+ could be determined. For each *k* measurement, at least four different mixing ratios of the volumetric mixtures were used. The rate constants for the reactions with NO^+ and $O_2^{\bullet+}$ were then determined in a relative way, as described in a previous paper [33] and as used in previous studies by Španěl et al. [20].

To determine the product ion distribution of the ion/molecule reactions studied, a removable reactant gas inlet is used, which is located at 8 mm from the ion inlet plate to reduce diffusion enhancement effects to a minimum [34]. MVK, MaCR, pivaldehyde, 2-methyl-butanal and glyoxal were introduced using volumetrically prepared mixtures in helium, whereas the tolualdehydes were injected in gaseous form by blowing helium over the liquid. Product ion distributions were obtained using the multi ion mode, where the ion mass spectrometer is tuned sequentially at a number of fixed masses and the corresponding count rate at those masses is measured.

Regular measurements with calibration gases were performed to eliminate mass discrimination effects [33].

Except for glyoxal, all chemicals were commercially available. MVK and MaCR were obtained from Aldrich (purity 99 and 95%, respectively). Pivaldehyde, *m*-, *p*-tolualdehyde, 2-methyl-butanal (Acros) and *o*-tolualdehyde (Fluka) had purities 98, 98, 99, 95 and >98%, respectively.

Glyoxal $C_2H_2O_2$ in monomeric form has been prepared from the hydrated trimer $C_6H_6O_6 \cdot 2H_2O$ using the method described by Horowitz et al. [35]. Its purity (≥98%) relatively to formaldehyde has been checked by absorption measurements in the UV. The pure monomer under the form of yellow crystals was stored at 195 K. For the preparation of the gaseous glyoxal/helium mixtures, the trap was heated up to temperatures ranging from 240 to 250 K, depending on the partial glyoxal pressure required in the glyoxal/helium mixture.

3. Results and discussion

3.1. Reaction rate constants

An overview of the experimental derived rate constants k_{exp} of the reactions of H_3O^+, NO^+ and $O_2^{\bullet +}$ with the various compounds is given in Table 1.

Absolute reaction rate constants of H_3O^+ have been measured by monitoring the signal of the precursor ion as a function of the concentration of the reactant gas in the flow tube. The reaction rate constants of NO^+ and $O_2^{\bullet +}$ were measured relatively with respect to the one of H_3O^+ by injecting the three precursor ions simultaneously and by recording their signal as a function of the concentration of the reactant gas. Exceptionally, the NO^+ and $O_2^{\bullet +}$ reactions with glyoxal were measured in an absolute way.

The accuracy of the experimental rate constants k_{exp} is estimated to be 20% with a precision better than 5% for the absolute measurements (except for glyoxal) and better than 2% for the relative measurements. The precision of the absolute measurements with glyoxal is better than 13%.

The corresponding collisional reaction rate constants k_C, obtained with the parameterized equation of Su and Chesnavich [39,40], are also listed in Table 1. The evaluation of k_C requires knowledge of the dipole moment μ_D and of the polarizability α of the reactants. Since literature data are sparse, these variables have been derived with the Gaussian software suite [41] at the B3LYP level of theory, using the extended

Table 1

Experimental rate constants k_{exp} obtained for the reactions of H_3O^+, $H_3O^+ \cdot H_2O$, NO^+, $NO^+ \cdot H_2O$ and $O_2^{\bullet +}$ with methyl vinyl ketone and some aldehydes at 150 Pa and 297 K

Compound	μ_D (Debye)	α (Å^3)	k_{exp} [k_C]				
			H_3O^+	$H_3O^+ \cdot H_2O$	NO^+	$NO^+ \cdot H_2O$	$O_2^{\bullet +}$
Methyl vinyl ketone	3.40 3.16[a]	8.23	3.5 [4.7]	3.7 [3.7]	2.4 [4.0]	3.5 [3.4]	3.0 [3.9]
o-Tolualdehyde	3.11	15.0	3.8 [4.4]	4.1 [3.3]	3.3 [3.6]	3.8 [3.0]	3.2 [3.5]
m-Tolualdehyde	3.63	15.1	4.1 [4.9]	4.7 [3.8]	3.6 [4.1]	4.6 [3.4]	3.6 [4.0]
p-Tolualdehyde	4.11	15.3	4.4 [5.5]	4.9 [4.2]	3.9 [4.6]	4.4 [3.8]	3.8 [4.4]
Pivaldehyde	2.87 2.66[b]	9.98	3.5 [4.0]	3.8 [3.1]	3.0 [3.4]	3.3 [2.9]	3.0 [3.3]
2-Methyl-butanal	3.11	10.1	3.7 [4.3]	3.9 [3.3]	3.2 [3.6]	3.3 [3.1]	3.1 [3.5]
Methacrolein	3.07 2.68[b]	8.32 8.3[b]	3.5 [4.3] [3.8]	3.8 [3.4] [3.0]	2.6 [3.6] [3.2]	3.4 [3.1] [2.8]	3.1 [3.6] [3.2]
trans-Glyoxal	0	4.75	1.9 [1.3]	–[d] [1.1]	0.08 [1.1]	– [1.0]	1.5 [1.1]
cis-Glyoxal	3.55 4.8[c]	4.76	[4.9]	[3.9]	[4.1]	[3.6]	[4.1]

In square brackets, collisional reaction rate constants k_C according to the Su and Chesnavich approach [39,40]. Polarizabilities α and dipole moments μ_D of the compounds obtained from quantum chemical calculations (see text for details) and from literature. k_{exp} and k_C are expressed in 10^{-9} cm^3 s^{-1}.

[a] Reference [36].

[b] Reference [37].

[c] Reference [38].

[d] See text at the end of Section 3.2.1.

Table 2
Product ion distribution of the H_3O^+, NO^+ and $O_2^{\bullet+}$ reactions with MVK and some aldehydes at 150 Pa He pressure and 297 K

Compound	*m*	PA	IE	H_3O^+				NO^+			$O_2^{\bullet+}$		
				Ion	*m/z*	%	k_2	Ion	*m/z*	%	Ion	*m/z*	%
Methyl vinyl ketone, $CH_2{=}CHCOCH_3$	70	834.7[b]	9.65[c]	$C_4H_7O^+$	71	99	2.3	$(NO\cdot C_4H_6O)^+$	100	99	$C_4H_6O^{\bullet+}$	70	49
				Others		1		Others		1	$C_3H_3O^+$	55	48
											$C_2H_3O^+$	43	2
											Others		1
o-Tolualdehyde, C_8H_8O	120			$C_8H_9O^+$	121	97	6.4	$C_8H_8O^{\bullet+}$	120	5	$C_8H_8O^{\bullet+}$	120	88
				Others		3		$C_8H_7O^+$	119	94	$C_8H_7O^+$	119	10
								Others		1	Others		2
m-Tolualdehyde, C_8H_8O	120	840.0[b]		$C_8H_9O^+$	121	98	6.4	$(NO\cdot C_8H_8O)^+$	150	5	$C_8H_8O^{\bullet+}$	120	88
				Others		2		$C_8H_8O^{\bullet+}$	120	6	$C_8H_7O^+$	119	11
								$C_8H_7O^+$	119	89	Others		1
p-Tolualdehyde, C_8H_8O	120	851.8[b]	9.33[d]	$C_8H_9O^+$	121	97	4.5	$(NO\cdot C_8H_8O)^+$	150	3	$C_8H_8O^{\bullet+}$	120	88
			9.34[e]	Others		3		$C_8H_8O^{\bullet+}$	120	4	$C_8H_7O^+$	119	11
								$C_8H_7O^+$	119	93	Others		1
Pivaldehyde, $C(CH_3)_3CHO$	86		9.51[c]	$C_5H_{11}O^+$	87	99	7.5	$(NO\cdot C_5H_{10}O)^+$	116	2	$C_5H_{10}O^{\bullet+}$	86	43
				Others		1		$C_5H_9O^+$	85	61	$C_4H_9^+$	57	56
								$C_4H_9^+$	57	37	Others		1
2-Methyl-butanal, $CH_3CH_2CH(CH_3)CHO$	86		9.59[f]	$C_5H_{11}O^+$	87	93	19	$C_5H_9O^+$	85	97	$C_5H_{10}O^{\bullet+}$	86	11
				$C_5H_9^+$	69	4	–[h]	$C_4H_9^+$ or $C_3H_5O^+$	57	2	$C_3H_6O^{\bullet+}$	58	70
				$C_2H_5O^+$	45	2	–[h]	Others		1	$C_4H_9^+$ or $C_3H_5O^+$	57	15
				Others		1					Others		4
3-Methyl-butanal[a], $CH_3CH(CH_3)CH_2CHO$	86		9.72[g]	$C_5H_{11}O^+$	87	70	12	$C_5H_9O^+$	85	100	$C_5H_{10}O^{\bullet+}$	86	10
				$C_5H_9^+$	69	30					$C_4H_7O^+$	71	10
											$C_3H_6O^{\bullet+}$	58	45
											$C_2H_4O^{\bullet+}$	44	35
Methacrolein, $CH_2{=}C(CH_3)CHO$	70	808.7[b]	9.92[g]	$C_4H_7O^+$	71	99	4.3	$(NO\cdot C_4H_6O)^+$	100	38	$C_4H_6O^{\bullet+}$	70	73
				Others		1		$C_4H_5O^+$	69	61	$C_4H_5O^+$	69	11
								Others		1	$C_3H_6^{\bullet+}$	42	14
											Others		2
Glyoxal, CHOCHO	58		10.2[c]	$C_2H_3O_2^+$	59	98	–[i]	$(NO\cdot C_2H_2O_2)^+$	88	100	$C_2H_2O_2^{\bullet+}$	58	49
				Others		2					$CH_2O^{\bullet+}$	30	48
											CHO^+	29	3

Three-body rate constants k_2 for the association of the protonated compounds with water in 10^{-27} cm^6 s^{-1}. Only product ions with a branching ratio ≥2% are listed. Product ions with smaller branching ratio are grouped together in “others”. *m*: mass of the compounds (u); PA: proton affinity (kJ mol^{-1}); IE: ionization energy (eV); %: branching ratio of the product ion, including all isotopes of the product, *m/z* value refers to the first isotope op the product ion.

[a] Reference [21].
[b] Reference [43].
[c] Reference [44].
[d] Reference [45].
[e] Reference [46].
[f] Reference [47].
[g] Reference [48].
[h] k_2 has only be determined for product ions with branching ratio ≥90% for reasons explained in Appendix A.
[i] See text at the end of Section 3.2.1.

aug-cc-pvdz basis set. Dipole moment μ_D and polarizability α are also listed in Table 1.

This table shows that the H_3O^+, NO^+ and $O_2^{\bullet+}$ reactions are fast, except the NO^+/glyoxal reaction. The k_{exp} values equal the corresponding collisional reaction rate constant k_C within the accuracy, with exception of the MVK reactions and the NO^+/MaCR reaction. A slight increase of the dipole moment μ_D is observed in the series *o*-, *m*- and *p*-tolualdehyde, which is reflected in a small increase of the corresponding k_{exp}.

k_C values for the *cis*- and *trans*-geometrical isomer of the dialdehyde glyoxal are quite different. The experimental value is closest to the calculated k_C value of the *trans*-geometry, which is the most stable isomer [42].

The values of the experimental reaction rate constants of $H_3O^+ \cdot H_2O$ and $NO^+ \cdot H_2O$ with the various reactants are also given in Table 1. They are derived in a relative way with respect to the reaction rate constant of H_3O^+ and NO^+, respectively, as explained in Appendix A. Comparison with the corresponding collisional reaction rate constants k_C, indicates that these reactions proceed at the collision rate and that the method outlined in Appendix A has the tendency to overestimate k_{exp} ($H_3O^+ \cdot H_2O$) and k_{exp} ($NO^+ \cdot H_2O$).

3.2. Product ion distributions

Table 2 gives an overview of the product ions observed in the reactions of H_3O^+, NO^+ and $O_2^{\bullet+}$ with the various compounds. These reactions are discussed in the following separate subparagraphs.

3.2.1. H_3O^+ reactions

All H_3O^+ reactions studied here proceed by proton transfer. This is expected for MVK, MaCR, *m*- and *p*-tolualdehyde from the large value of their proton affinity (see Table 2). It indicates that the proton affinity of the other products in Table 2 is also larger than the one of H_2O (691 kJ mol^{-1} [43]). In all cases, except for 2-methyl-butanal, this proton transfer process is non-dissociative, resulting in the protonated molecule as single reaction product:

$$H_3O^+ + M \rightarrow MH^+ + H_2O. \tag{1}$$

For 2-methyl-butanal, in addition to the protonated molecule, two other products are formed either by the loss of a H_2O molecule or by elimination of C_3H_6 after protonation:

$$H_3O^+ + CH_3CH_2CH(CH_3)CHO \rightarrow C_5H_{11}O^+ + H_2O \tag{2.1}$$

$$H_3O^+ + CH_3CH_2CH(CH_3)CHO \rightarrow C_5H_9{}^+ + 2H_2O \tag{2.2}$$

$$H_3O^+ + CH_3CH_2CH(CH_3)CHO \rightarrow C_2H_5O^+ + C_3H_6 + H_2O. \tag{2.3}$$

Španěl et al. [20,21] observed elimination of a water molecule after protonation for saturated aldehydes containing at least four carbon atoms (except for 2-methyl-propanal). By analogy with electron ionization fragmentation EI [49,50], they suggested that a possible mechanism for the H_2O elimination involves the formation of a six-membered ring intermediate containing at least four carbon atoms. Our study seems to support this hypothesis: pivaldehyde cannot form a six-membered cyclic intermediate and the water elimination channel should not take place, which is indeed observed. On the other hand, the formation of such an intermediate is possible for 2-methyl-butanal and water elimination (see reaction (2.2)) is observed.

In their study of the reaction of H_3O^+ with an extended series of ketones Smith and co-workers [20,22] concluded that these reactions are characterized by non-dissociative proton transfer as single reaction pathway, which is confirmed by the H_3O^+/MVK reaction in this study:

$$H_3O^+ + CH_2{=}\,CHC(O)CH_3 \rightarrow C_4H_7O^+ + H_2O. \tag{3}$$

Several SIFT studies [51–53] have revealed that association of water molecules to hydrocarbon ions is generally exceptional and that hydrocarbons do not react significantly with hydrated hydronium ions by switching reactions. These properties can be used as a valuable diagnostic tool in determining the nature of the reaction products. For example, the product ion at $m/z = 45$ in reaction (2.3) hydrates when water is added to the main carrier gas, so it is most likely identified as the oxygen bearing ion $C_2H_5O^+$, rather than the hydrocarbon ion $C_3H_9{}^+$. We have used this tool in all further cases where identification of the product ions was doubtful.

For all H_3O^+ reaction products listed in Table 2, except for protonated glyoxal, association with water takes place. Higher order hydrates are formed, except for protonated *o*-, *m*- and *p*-tolualdehyde for which only the monohydrate was observed. The three-body association rate constants, as derived by the method described in Appendix A, are also included in Table 2.

The reaction of protonated glyoxal with water is peculiar: when water is added to the main carrier gas, the signal of protonated glyoxal decreases significantly, but an equivalent increase of the signals of the hydrates of protonated glyoxal is not recorded. On the other hand, a distinct increase of the signal at $m/z = 31$ (most likely protonated formaldehyde H_2COH^+ and not its much higher energy isomer CH_3O^+) and of its hydrate at $m/z = 49$ ($H_2COH^+ \cdot H_2O$), which are only minor products with branching ratio ≤1% in the absence of water, is observed. When the concentration of glyoxal in the reaction zone is increased for a fixed water vapor concentration, an unexpected increase of the signal at $m/z = 37$ is also observed, which can possibly be explained by the following reaction:

$$C_2H_3O_2{}^+ \cdot H_2O + H_2O \rightarrow H_3O^+ \cdot H_2O + C_2H_2O_2. \tag{4}$$

It is clear that further experiments are needed to unravel the complex H_3O^+/glyoxal chemistry in the presence of water vapor.

3.2.2. NO^+ reactions

For most products in Table 2 the ionization energy IE is known and is larger than the one of NO (IE(NO) = 9.26 eV [44]), so charge transfer with ground state NO^+ is excluded (except for *p*-tolualdehyde, see later on).

MVK reacts with NO^+ through association at an effective bimolecular reaction rate, which is under our SIFT conditions about 40% lower than the corresponding collision rate constant k_C (see Table 1):

$$NO^+ + CH_2 = CHC(O)CH_3 \xrightarrow{He} (NO \cdot C_4H_6O)^+. \qquad (5)$$

Based upon their study of an extensive series of ketones, Smith and co-workers [20,22] concluded that for most of the ketones they have studied, association is the only or dominant pathway in their reaction with NO^+, in accordance with the observed reaction (5) for MVK.

Association is also the only process observed in the NO^+/glyoxal reaction, however at a very small effective bimolecular reaction rate (see Table 1):

$$NO^+ + CHOCHO \xrightarrow{He} (NO \cdot C_2H_2O_2)^+. \qquad (6)$$

Further studies as a function of the pressure would be useful to probe the variation of the rate constant.

The major process for the reaction of NO^+ with the monoaldehydes listed in Table 2 is hydride ion transfer. Hydride ion transfer has been identified by Španěl et al. [20,21] as the only process occurring in the reaction of NO^+ with saturated aldehydes and as the dominant pathway for the reaction of NO^+ with unsaturated aldehydes.

In addition to hydride ion transfer (reaction (7.3)), two less important processes are observed in the NO^+/tolualdehyde (*o*-, *m*- and *p*-) reaction:

$$NO^+ + C_8H_8O \xrightarrow{He} (NO \cdot C_8H_8O)^+ \qquad (7.1)$$

$$NO^+ + C_8H_8O \rightarrow C_8H_8O^{\bullet +} + NO \qquad (7.2)$$

$$NO^+ + C_8H_8O \rightarrow C_8H_7O^+ + HNO. \qquad (7.3)$$

The branching ratio for the *o*-tolualdehyde/NO^+ association reaction (7.1) is smaller than 1.5%. The charge transfer channel (7.2) is somewhat surprising for the NO^+/*p*-tolualdehyde reaction, since the ionization energy of *p*-tolualdehyde (see Table 2) is larger than the one of NO. These charge transfer products cannot originate from excited $NO^{+,*}$ precursor ions, because these ions have been quenched during the experiments by adding a small amount of N_2 to the He main carrier gas. However, if one takes into account the uncertainty on the ionization energy, the thermal spread of the ion/molecule interaction energies under SIFT conditions and the possible entropy change ($T\Delta S$ typical $\leq 6.3\ kJ\ mol^{-1}$ for bimolecular reactions [54]), charge transfer with ground state NO^+ is not excluded. Charge transfer has indeed been observed for the reaction of NO^+ with ethylene glycol dimethyl ether [55], 1-heptene, 1-octene, 1-nonene, 1-decene [53] and acetophenone [22], all molecules with IE slightly larger than NO.

For the NO^+/pivaldehyde reaction three products have been identified:

$$NO^+ + C(CH_3)_3CHO \xrightarrow{He} (NO \cdot C_5H_{10}O)^+ \qquad (8.1)$$

$$NO^+ + C(CH_3)_3CHO \rightarrow C_5H_9O^+ + HNO \qquad (8.2)$$

$$NO^+ + C(CH_3)_3CHO \rightarrow C_4H_9{}^+ + (CHO + NO). \qquad (8.3)$$

The major channel (8.2) corresponds to hydride ion transfer and pathway (8.3) leads to the hydrocarbon ion $C_4H_9{}^+$ by elimination of CHO. In the latter reaction, several neutral products may be possible. However, since thermodynamic data are missing to trace the energetics of the reactions, these neutral products cannot be specified exactly. Therefore, we have put in (8.3), between brackets, the neutral products of the reaction as consisting of the molecule emanating from the source ion and of the fragment coming from the neutral reaction partner. From now on, we will use the same notation (brackets for uncertain neutral reaction products) in the discussion below.

The major channel in the NO^+/2-methyl-butanal reaction is again hydride ion transfer (9.1), with one minor channel:

$$NO^+ + CH_3CH_2CH(CH_3)CHO \rightarrow C_5H_9O^+ + HNO \qquad (9.1)$$

$$NO^+ + CH_3CH_2CH(CH_3)CHO \rightarrow C_4H_9{}^+ + (CHO + NO) \text{ or} \qquad (9.2.1)$$

$$NO^+ + CH_3CH_2CH(CH_3)CHO \rightarrow C_3H_5O^+ + (C_2H_5 + NO). \qquad (9.2.2)$$

The minor product at *m*/*z* = 57 could be $C_4H_9{}^+$ (protonated 1-butene, 2-butene or isobutene, reaction (9.2.1)) or $C_3H_5O^+$ (reaction (9.2.2)). Diskin et al. [53] observed that protonated 1-pentene, protonated *trans*-2-pentene and higher order protonated alkenes (double bound in the 1 or 2 position) do not associate significantly with water. Since this series does not include protonated butene, association of the latter with water cannot be ruled out a priori. Furthermore, when water is introduced into the flow tube, the signal at *m*/*z* = 57 ($C_4H_9{}^+$ or $C_3H_5O^+$) decreases significantly, but this decrease is not mirrored in an equivalent increase of the signals of the hydrates at *m*/*z* = 75 ($C_4H_9{}^+\cdot H_2O$ or $C_3H_5O^+\cdot H_2O$), *m*/*z* = 93 ($C_4H_9{}^+\cdot(H_2O)_2$ or $C_3H_5O^+\cdot(H_2O)_2$) and *m*/*z* = 111 ($C_4H_9{}^+\cdot(H_2O)_3$ or $C_3H_5O^+\cdot(H_2O)_3$). It is clear that the nature of the minor product at *m*/*z* = 57 remains uncertain and that the chemistry, when water is added to the main carrier gas, needs further investigation.

Finally, the two products of the NO^+/MaCR reaction can be explained by association (10.1) and hydride ion transfer (10.2):

$$NO^+ + CH_2 = C(CH_3)CHO \xrightarrow{He} (NO \cdot C_4H_6O)^+ \qquad (10.1)$$

$$NO^+ + CH_2 = C(CH_3)CHO \rightarrow C_4H_5O^+ + HNO. \qquad (10.2)$$

The same reaction pathways have been observed in the reaction of NO^+ with the related compound acrolein [20].

For all the ion products of the NO^+ reactions listed, including the $(M-H)^+$ ions resulting from hydride ion transfer, no or only minor hydrates have been observed, when water is added to the main carrier gas (except the charge transfer product at $m/z = 120$ for the NO^+/*o*-tolualdehyde reaction, see also Section 3.2.3).

3.2.3. $O_2^{\bullet+}$ reactions

All $O_2^{\bullet+}$ reactions can be characterized as charge transfer, resulting in the parent cation and in at least one fragment (in some cases hydride or methide ion transfer or other transfer reactions cannot be excluded).

The $O_2^{\bullet+}$/MVK reaction results in the parent cation and two fragments, due to the elimination of the methyl and vinyl radical:

$$O_2^{\bullet+} + CH_2 = CHC(O)CH_3 \rightarrow C_4H_6O^{\bullet+} + O_2 \qquad (11.1)$$

$$O_2^{\bullet+} + CH_2 = CHC(O)CH_3 \rightarrow C_3H_3O^+ + (CH_3 + O_2) \qquad (11.2)$$

$$O_2^{\bullet+} + CH_2 = CHC(O)CH_3 \rightarrow C_2H_3O^+ + (C_2H_3 + O_2). \qquad (11.3)$$

In the reactions of $O_2^{\bullet+}$ with *o*-, *m*- and *p*-tolualdehyde, we observe non-dissociative charge transfer as major process, next to elimination of an H atom:

$$O_2^{\bullet+} + C_8H_8O \rightarrow C_8H_8O^{\bullet+} + O_2 \qquad (12.1)$$

$$O_2^{\bullet+} + C_8H_8O \rightarrow C_8H_7O^+ + (H + O_2). \qquad (12.2)$$

The branching ratio of these processes is the same for the three isomers.

The $O_2^{\bullet+}$/pivaldehyde reaction gives rise to the parent cation and to a hydrocarbon product ion at $m/z = 57$ ($C_4H_9^+$), most likely a tertiary butyl cation:

$$O_2^{\bullet+} + C(CH_3)_3CHO \rightarrow C_5H_{10}O^{\bullet+} + O_2 \qquad (13.1)$$

$$O_2^{\bullet+} + C(CH_3)_3CHO \rightarrow C_4H_9^+ + (CHO + O_2). \qquad (13.2)$$

The $O_2^{\bullet+}$/2-methyl-butanal reaction proceeds through three channels:

$$O_2^{\bullet+} + CH_3CH_2CH(CH_3)CHO \rightarrow C_5H_{10}O^{\bullet+} + O_2 \qquad (14.1)$$

$$O_2^{\bullet+} + CH_3CH_2CH(CH_3)CHO \rightarrow C_3H_6O^{\bullet+} + (C_2H_4 + O_2) \qquad (14.2)$$

$$O_2^{\bullet+} + CH_3CH_2CH(CH_3)CHO \rightarrow C_4H_9^+ + (CHO + O_2) \text{ or} \qquad (14.3.1)$$

$$O_2^{\bullet+} + CH_3CH_2CH(CH_3)CHO \rightarrow C_3H_5O^+ + (C_2H_5 + O_2). \qquad (14.3.2)$$

By analogy with well understood EI fragmentation spectra, products at $m/z = 58$ (reaction (14.2)) are characteristic for α-methyl substituted aldehydes, resulting from H-rearrangement through a six-membered intermediate ring followed by β-cleavage [49]. Moreover, elimination of ethylene (reaction (14.2)) has been observed in many SIFT $O_2^{\bullet+}$ [20,21] and EI spectra of aldehydes [49]. The nature of the product ion in reactions (14.3.1) and (14.3.2) is uncertain for the same reasons as mentioned in the discussion of the NO^+/2-methyl-butanal reaction. A secondary butyl cation is most likely formed in reaction (14.3.1). Note that the product ion distribution for 3-methyl-butanal, measured by Španěl et al. [21], is also listed in Table 2. This distribution is quite different from the one of its structural isomer (products at $m/z = 44$ ($C_2H_4O^{\bullet+}$) and $m/z = 71$ ($C_4H_7O^+$) for 3-methyl-butanal, at $m/z = 57$ ($C_4H_9^+$ or $C_3H_5O^+$) for 2-methyl-butanal).

Non-dissociative charge transfer and elimination of an H atom and a CO molecule have been observed in the $O_2^{\bullet+}$/MaCR reaction:

$$O_2^{\bullet+} + CH_2 = C(CH_3)CHO \rightarrow C_4H_6O^{\bullet+} + O_2 \qquad (15.1)$$

$$O_2^{\bullet+} + CH_2 = C(CH_3)CHO \rightarrow C_4H_5O^+ + (H + O_2) \qquad (15.2)$$

$$O_2^{\bullet+} + CH_2 = C(CH_3)CHO \rightarrow C_3H_6^{\bullet+} + (CO + O_2). \qquad (15.3)$$

The same reaction pathways have been identified in the $O_2^{\bullet+}$/acrolein reaction [20].

The parent cation and the $CH_2O^{\bullet+}$ fragment ion, due to the ejection of a CO molecule, are the major product ions for the reaction of $O_2^{\bullet+}$ with glyoxal. A minor product ion CHO^+ results from the cleavage of the C–C bond:

$$O_2^{\bullet+} + CHOCHO \rightarrow C_2H_2O_2^{\bullet+} + O_2 \qquad (16.1)$$

$$O_2^{\bullet+} + CHOCHO \rightarrow CH_2O^{\bullet+} + (CO + O_2) \qquad (16.2)$$

$$O_2^{\bullet+} + CHOCHO \rightarrow CHO^+ + (CHO + O_2). \qquad (16.3)$$

When water is introduced in the main carrier gas, major hydrates of only a few $O_2^{\bullet+}$ reaction product ions are observed: i.e., the product at $m/z = 58$ for 2-methyl-butanal and the charge transfer products of MVK, of tolualdehyde in its *o*-configuration (only monohydrate) and of MaCR. The signal of the charge transfer products of pivaldehyde and 2-methyl-butanal and of all products of the $O_2^{\bullet+}$/glyoxal reaction decrease significantly when water vapor is present, but the signal of the corresponding hydrates does not rise equivalently.

4. Conclusion

All H_3O^+, $H_3O^+{\cdot}H_2O$, NO^+, $NO^+{\cdot}H_2O$ and $O_2^{\bullet+}$ reactions studied are fast and proceed close to the collision rate, except the NO^+/glyoxal reaction. General trends in the chemistry of the reactions of H_3O^+, NO^+ and $O_2^{\bullet+}$ with ketones and aldehydes under SIFT conditions, observed by Španěl and co-workers [20–22] have been confirmed in this study.

We conclude that none of the three precursor ions is suitable to distinguish the three isomeric forms of tolualdehyde, since in all cases the branching ratios of the product ions are similar. For the H_3O^+/tolualdehyde reactions, the major product is $C_8H_9O^+$, for the NO^+/tolualdehyde reactions hydride ion transfer is dominant giving $C_8H_7O^+$ product ions and for the $O_2^{\bullet+}$/tolualdehyde reactions the major pathway is charge transfer resulting in $C_8H_8O^{\bullet+}$ ions.

NO^+ is suitable to discriminate the two structural isomers MVK/MaCR, based upon the product at $m/z = 69$, corresponding with a hydride ion transfer mechanism resulting in $C_4H_5O^+$ product ions, which is only observed for MaCR. On the other hand, product ions at $m/z = 55$ ($C_3H_3O^+$), corresponding with the elimination of a methyl radical, and at $m/z = 69$ ($C_4H_5O^+$), due to the elimination of an H atom, are useful for this purpose, when $O_2^{\bullet+}$ is the primary ion.

In a similar way, the intensity of the products at $m/z = 44$, 57, 58 and 71 with $O_2^{\bullet+}$ as precursor ion can be used to distinguish the three structural isomers pivaldehyde, 2- and 3-methyl-butanal.

To examine the application of the ion chemistry studied here, under conditions where water plays an important role, we have investigated further hydration of the reaction products as well as the reaction of the neutrals with $H_3O^+{\cdot}H_2O$ and $NO^+{\cdot}H_2O$. A method to estimate the reaction rate constants of $H_3O^+{\cdot}H_2O$ and $NO^+{\cdot}H_2O$ with neutral reactants and of the three-body association of product ions with water is proposed.

In a few cases, for example, for glyoxal, the chemistry involved when water vapor is introduced in the reaction zone, remains unclear and needs further investigation.

Acknowledgements

We thank Dr. Labonnette (LPCE-CNRS) for his support in the preparation of the glyoxal samples.

This work was partly funded by the Belgian “Federal Office for Scientific, Technical and Cultural Affairs” within the framework of the “Scientific support plan for a sustainable development policy (SPSD 2) – Global change, ecosystems and biodiversity – Project EV/35/06”.

Appendix A

Given the reaction of the precursor ion H_3O^+ with the reactant gas M:

$$H_3O^+ + M \rightarrow MH^+ + H_2O \qquad (A.1.1)$$

$$H_3O^+ + M \rightarrow \text{other products.} \qquad (A.1.2)$$

When water vapor is added to the He carrier gas the product ions MH^+ may partially associate with water to form the monohydrate $MH^+{\cdot}H_2O$:

$$MH^+ + H_2O \xrightarrow{He} MH^+ \cdot H_2O. \qquad (A.2)$$

The precursor ions H_3O^+ also partially cluster with water:

$$H_3O^+ + H_2O \xrightarrow{He} H_3O^+ \cdot H_2O. \qquad (A.3)$$

Successive three-body association reactions result in higher order hydrates $H_3O^+{\cdot}(H_2O)_n$ and $MH^+{\cdot}(H_2O)_n$, as depicted in Scheme 1.

The hydrated hydronium ions $H_3O^+{\cdot}(H_2O)_{1,2,3}$ may behave as additional precursor ions, reacting with the reactant gas M by ligand switching. For example:

$$H_3O^+ \cdot H_2O + M \rightarrow MH^+ + 2H_2O \qquad (A.4.1)$$

$$H_3O^+ \cdot H_2O + M \rightarrow MH^+ \cdot H_2O + H_2O. \qquad (A.4.2)$$

In the limiting case of very low water vapor concentrations, the extended set of ions in Scheme 1 can be restricted to

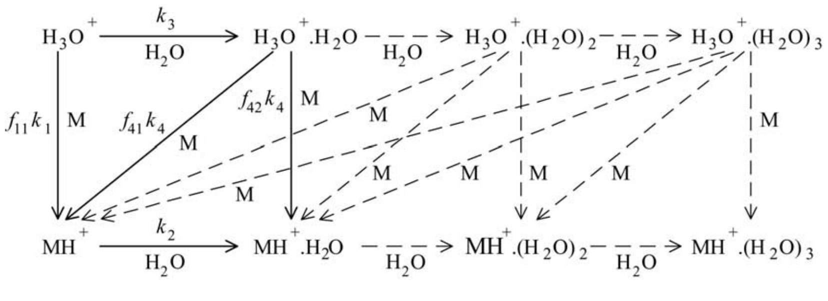

Scheme 1.

$H_3O^+ \cdot (H_2O)_{0,1}$ and $MH^+ \cdot (H_2O)_{0,1}$. By solving the set of coupled differential equations (describing the kinetics of these ions), one can show that in the limiting case of very low concentration of the reactant gas M, the ratio of the rate constant k_4 of the reaction of $H_3O^+ \cdot H_2O$ with M and the known rate constant k_1 of the reaction of H_3O^+ with M, is given by:

$$\frac{k_4}{k_1} = \frac{2\ln\left(\frac{[H_3O^+ \cdot H_2O]_0}{[H_3O^+ \cdot H_2O]}\right)}{\ln\left(\frac{[H_3O^+]_0}{[H_3O^+]}\right)} - 1, \tag{A.5}$$

where subscript '0' refers to count rates in the absence of the reactant gas M. It is assumed that the water vapor and the reactant gas are introduced at the same distance from the detector quadrupole. In our set-up, the reactant gas/helium mixture and the water vapor are injected in the buffer gas flow by the same ring-shaped inlet, located at 27 cm from the quadrupole inlet plate. Experimentally the ion signal of H_3O^+ (=x) and of $H_3O^+ \cdot H_2O$ (=y) is monitored for several small concentrations of the reactant gas M and for a fixed small concentration of water vapor. Linear regression of the data points $2 \times \ln(y_0/y)$ versus $\ln(x_0/x)$ allows us to derive k_4/k_1 according to Eq. (A.5).

The ratio of the three-body rate constants k_2 and k_3 for the association of MH^+ and H_3O^+ with water is given by:

$$\frac{k_2}{k_3} = \frac{2\ln\left(\frac{[MH^+]_1}{[MH^+]}\right)}{\ln\left(\frac{[H_3O^+]_1}{[H_3O^+]}\right)} + \frac{f_{41}k_4}{f_{11}k_1} - 1, \tag{A.6}$$

k_3 was measured by [56] at 298 K and at a helium buffer gas pressure of 93 Pa and equals 5.8×10^{-28} cm^6 s^{-1}. It is supposed that the 150 Pa pressure in the flow tube of our SIFT apparatus is inside the pressure range where the effective bimolecular reaction rate constant varies linearly with pressure. f_{11} and f_{41} are the branching ratios of MH^+ for the reaction of M with H_3O^+ and $H_3O^+ \cdot H_2O$, respectively. Subscript '1' now refers to count rates in the absence of water.

However, our SIFT apparatus does not allow an accurate measurement of the product ion distribution of the $H_3O^+ \cdot H_2O$/M reaction (f_{41} and f_{42}). When the injection quadrupole is tuned for $H_3O^+ \cdot H_2O$, almost all precursor ions detected are H_3O^+ ions, probably due to break-up of the $H_3O^+ \cdot H_2O$ ions at the injection point. Consequently, the ion concentration of $H_3O^+ \cdot H_2O$ in the reaction zone is too low for an accurate determination of the product ion distribution of $H_3O^+ \cdot H_2O$ and to distinguish the latter from the one of H_3O^+.

If MH^+ is the major product ion of reactions (A.1.1) and (A.1.2) ($f_{11} \sim 1$), the term $(f_{41}k_4)/(f_{11}k_1)$ in Eq. (A.6) is at most ∼1. In this case, neglecting this term in Eq. (A.6) will introduce an error of maximum ∼1 on the ratio k_2/k_3. Therefore, if the product ion distribution of $H_3O^+ \cdot H_2O$ is not known, the error on k_2/k_3 due to the omission of the term $(f_{41}k_4)/(f_{11}k_1)$ in Eq. (A.6), will certainly be minimal for major product ions (branching ratio ≥90%). Experimentally the signals of the H_3O^+ (=x) and MH^+ (=y) ions are determined for several small water vapor concentrations and for a fixed small concentration of the reactant gas M. A polynomial fit of the $2 \times \ln(y_1/y)$ versus $\ln(x_1/x)$ data points gives us k_2/k_3 according to Eq. (A.6).

A similar argumentation holds for NO^+ and its hydrate $NO^+ \cdot H_2O$: the ratio of the rate constant of the reaction of $NO^+ \cdot H_2O$ with the reactant M and the one of NO^+ is given by an equation similar to Eq. (A.5).

It should be noted that in Eqs. (A.5) and (A.6) effects of mass discrimination cancel out, but in the derivation of these equations ion diffusion and subsequent loss on the flow tube wall was not taken into account. In order to estimate the effect of differential diffusion (low molecular mass ions diffuse faster than high molecular mass ions) on k_4/k_1 and k_2/k_3 obtained with Eqs. (A.5) and (A.6), respectively, the rate equations of reactions (A.1.1)–(A.4.2) with additional ion diffusion loss terms were solved numerically, using a finite difference method. Recently reported theoretical reduced ion mobility data [57] were used to calculate the diffusion coefficients in our experimental SIFT conditions. The model calculations have shown that, due to diffusion enhancement [34], the values for k_4/k_1 obtained with Eq. (A.5) are underestimated by some 3%, whereas the values for k_2/k_3 obtained with Eq. (A.6) may be overestimated by 10% for neutral reactants with a molecular mass of about 50 u, and even by 15% for reactants of molecular mass 140 u.

References

[1] R. Atkinson, Atmos. Environ. 34 (2000) 2063.
[2] M. Jang, R.M. Kamens, Environ. Sci. Technol. 35 (2001) 4758.
[3] M. Stupfel, Environ. Health Perspect. 17 (1976) 253.
[4] D.W.M. Sin, Y.-C. Wong, P.K.K. Louie, Atmos. Environ. 35 (2001) 5961.
[5] J.-F. Müller, J. Geophys. Res. 97 (1992) 3787.
[6] R. Holzinger, C. Warneke, A. Hansel, A. Jordan, W. Lindinger, Geophys. Res. Lett. 26 (1999) 1161.
[7] A. Kristensson, C. Johansson, R. Westerholm, E. Swietlicki, L. Gidhagen, U. Wideqvist, V. Vesely, Atmos. Environ. 38 (2004) 657.
[8] P. Carlier, H. Hannachi, G. Mouvier, Atmos. Environ. 20 (1986) 2079.
[9] R. Atkinson, J. Arey, Atmos. Environ. 37 (2) (2003) S197.
[10] H.B. Singh, L.J. Salas, R.B. Chatfield, E. Czech, A. Fried, J. Walega, M.J. Evans, B.D. Field, D.J. Jacob, D. Blake, B. Heikes, R. Talbot, G. Sachse, J.H. Crawford, M.A. Avery, S. Sandholm, H. Fuelberg, J. Gepohys. Res. 109 (2004) D15S07, doi:10.1029/2003JD003883.
[11] A. Guenther, C.N. Hewitt, D. Erikson, R. Fall, C. Geron, T. Graedel, P. Harley, L. Klinger, M. Lerdau, W.A. McKay, T. Pierce, B. Scholes, R. Steinbrecher, R. Tallamraju, J. Taylor, P. Zimmerman, J. Geophys. Res. 100 (1995) 8873.
[12] A. Guenther, C. Geron, T. Pierce, B. Lamb, P. Harley, R. Fall, Atmos. Environ. 34 (2000) 2205.
[13] J.A. de Gouw, P.D. Goldan, C. Warneke, W.C. Kuster, J.M. Roberts, M. Marchewka, S.B. Bertman, A.A.P. Pszenny, W.C. Keene, J. Geophys. Res. 108 (D21) (2003) 4682, doi:10.1029/2003JD003863.
[14] P. Španěl, D. Smith, Med. Biol. Eng. Comput. 34 (1996) 409.
[15] D. Smith, P. Španěl, J.M. Thompson, B. Rajan, J. Cocker, P. Rolfe, Appl. Occup. Environ. Hyg. 13 (1998) 817.
[16] P. Španěl, S. Davies, D. Smith, Rapid Commun. Mass Spectrom. 13 (1999) 1733.

[17] P. Španěl, A.M. Diskin, S.M. Abbott, T. Wang, D. Smith, Rapid Commun. Mass Spectrom. 16 (2002) 2148.
[18] S.M. Abbott, J.B. Elder, P. Španěl, D. Smith, Int. J. Mass Spectrom. 228 (2003) 655.
[19] V.G. Anicich, An Index of the Literature for Bimolecular Gas Phase Cation-Molecule Reaction Kinetics, JPL Publication 03-19, National Aeronautics and Space Administration, Jet Propulsion Laboratory, California Institute of Technology, Pasadena, California, United States, November 2003, http://techreports.jpl.nasa.gov/2003/03-2964.pdf.
[20] P. Španěl, Y. Ji, D. Smith, Int. J. Mass Spectrom. Ion Process. 165/166 (1997) 25.
[21] P. Španěl, J.M. Van Doren, D. Smith, Int. J. Mass Spectrom. 213 (2002) 163.
[22] D. Smith, T. Wang, P. Španěl, Rapid Commun. Mass Spectrom. 17 (2003) 2655.
[23] M. Jang, R.M. Kamens, Environ. Sci. Technol. 35 (2001) 3626.
[24] E.C. Tuazon, R. Atkinson, H. Mac Leod, H.W. Biermann, A.M. Winer, W.P.L. Carter, J.N. Pitts Jr., Environ. Sci. Technol. 18 (1984) 981.
[25] J. Yu, H.E. Jeffries, K.G. Sexton, Atmos. Environ. 31 (1997) 2261.
[26] D.F. Smith, T.E. Kleindienst, C.D. McIver, J. Atmos. Chem. 34 (1999) 339.
[27] J. Yu, H.E. Jeffries, R.M. Le Lacheur, Environ. Sci. Technol. 29 (1995) 1923.
[28] J. Fick, L. Pommer, C. Nilsson, B. Andersson, Atmos. Environ. 37 (2003) 4087.
[29] A.J. Kean, E. Grosjean, D. Grosjean, R.A. Harley, Environ. Sci. Technol. 35 (2001) 4198.
[30] M.F. Mohamed, D. Kang, V.P. Aneja, Chemosphere 47 (2002) 863.
[31] H. Bandow, N. Washida, H. Akimoto, Bull. Chem. Soc. Jpn. 58 (1985) 2541.
[32] D. Smith, N.G. Adams, Adv. Atom. Mol. Phys. 24 (1988) 1.
[33] N. Schoon, C. Amelynck, L. Vereecken, E. Arijs, Int. J. Mass Spectrom. 229 (2003) 231.
[34] P. Španěl, D. Smith, J. Am. Soc. Mass Spectrom. 12 (2001) 863.
[35] A. Horowitz, R. Meller, G.K. Moortgat, J. Photochem. Photobiol. A: Chem. 146 (2001) 19.
[36] R.C. Weast (Editor-in-Chief), M.J. Astle, W.H. Beyer (Associate Editors), CRC Handbook of Chemistry and Physics, 64th ed., CRC Press Inc., Boca Raton, FL, USA, 1983–1984.
[37] D.R. Lide (Editor-in-Chief), CRC Handbook of Chemistry and Physics, 80th ed., CRC Press Inc., Boca Raton, FL, USA, 1999–2000.
[38] J.R. Durig, C.C. Tong, Y.S. Li, J. Chem. Phys. 57 (1972) 4425.
[39] T. Su, W.J. Chesnavich, J. Chem. Phys. 76 (1982) 5183.
[40] T. Su, J. Chem. Phys. 89 (1988) 5355.
[41] M.J. Frisch, G.W. Trucks, H.B. Schlegel, G.E. Scuseria, M.A. Robb, J.R. Cheeseman, V.G. Zakrzewski, J.A. Montgomery Jr., R.E. Stratmann, J.C. Burant, S. Dapprich, J.M. Millam, A.D. Daniels, K.N. Kudin, M.C. Strain, O. Farkas, J. Tomasi, V. Barone, M. Cossi, R. Cammi, B. Mennucci, C. Pomelli, C. Adamo, S. Clifford, J. Ochterski, G.A. Petersson, P.Y. Ayala, Q. Cui, K. Morokuma, D.K. Malick, A.D. Rabuck, K. Raghavachari, J.B. Foresman, J. Cioslowski, J.V. Ortiz, A.G. Baboul, B.B. Stefanov, G. Liu, A. Liashenko, P. Piskorz, I. Komaromi, R. Gomperts, R.L. Martin, D.J. Fox, T. Keith, M.A. Al-Laham, C.Y. Peng, A. Nanayakkara, C. Gonzalez, M. Challacombe, P.M.W. Gill, B. Johnson, W. Chen, M.W. Wong, J.L. Andres, C. Gonzalez, M. Head-Gordon, E.S. Replogle, J.A. Pople, Gaussian 98, Revision A.7, Gaussian Inc., Pittsburgh, PA, 1998.
[42] F. Bulat, A. Toro-Labbé, Chem. Phys. Lett. 354 (2002) 508.
[43] E.P. Hunter, S.G. Lias, in: P.J. Linstrom, W.G. Mallard (Eds.), Proton Affinity Evaluation in NIST Chemistry WebBook, NIST Standard Reference Database Number 69, National Institute of Standards and Technology, Gaithersburg, MD 20899, March 2003, http://webbook.nist.gov.
[44] S.G. Lias, in: P.J. Linstrom, W.G. Mallard (Eds.), Ionization Energy Evaluation in NIST Chemistry WebBook, NIST Standard Reference Database Number 69, National Institute of Standards and Technology, Gaithersburg, MD 20899, March 2003, http://webbook.nist.gov.
[45] H.M. Rosenstock, K. Draxl, B.W. Steiner, J.T. Herron, in: P.J. Linstrom, W.G. Mallard (Eds.), Ion Energetics Data in NIST Chemistry WebBook, NIST Standard Reference Database Number 69, National Institute of Standards and Technology, Gaithersburg, MD 20899, March 2003, http://webbook.nist.gov.
[46] S.G. Lias, J.E. Bartmess, J.F. Liebman, J.L. Holmes, R.D. Levin, W.G. Mallard, in: P.J. Linstrom, W.G. Mallard (Eds.), Ion Energetics Data in NIST Chemistry WebBook, NIST Standard Reference Database Number 69, National Institute of Standards and Technology, Gaithersburg, MD 20899, March 2003, http://webbook.nist.gov.
[47] R. Hernandez, P. Masclet, G. Mouvier, J. Electron. Spectrosc. Relat. Phenom. 10 (1977) 333.
[48] S.G. Lias, R.D. Levin, S.A. Kafafi, in: P.J. Linstrom, W.G. Mallard (Eds.), Ion Energetics Data in NIST Chemistry WebBook, NIST Standard Reference Database Number 69, National Institute of Standards and Technology, Gaithersburg, MD 20899, March 2003, http://webbook.nist.gov.
[49] H. Budzikiewicz, C. Djerassi, D.H. Williams, Interpretation of Mass Spectra of Organic Compounds, Holden-Day, San Francisco, 1964.
[50] F.W. McLafferty, F. Tureček, Interpretation of Mass Spectra, fourth ed., University Science Books, Sausalito, CA, 1993.
[51] P. Španěl, D. Smith, J. Phys. Chem. 99 (1995) 15551.
[52] P. Španěl, D. Smith, Rapid Commun. Mass Spectrom. 14 (2000) 1898.
[53] A.M. Diskin, T. Wang, D. Smith, P. Španěl, Int. J. Mass Spectrom. 218 (2002) 87.
[54] M. Henchman, Entropy-driven reactions: summary of the panel discussion in structure/reactivity and thermochemistry of ions, in: P. Ausloos, S.G. Lias (Eds.), NATO ASI Series, Series C: Mathematical and Physical Sciences, vol. 193, D. Reidel Publishing Company, Dordrecht, Holland, 1987.
[55] P. Španěl, D. Smith, Int. J. Mass Spectrom. Ion Process. 172 (1998) 239.
[56] D. Smith, P. Španěl, Rapid Commun. Mass Spectrom. 15 (2001) 563.
[57] K. Dryahina, P. Španěl, in: J. Safrankova (Ed.), WDS'04 Proceedings of Contributed Papers: Part II—Physics of Plasmas and Ionized Media, MATFYZPRESS, Prague, Czech Republic, 2004, pp. 407–412.